

Identification of differentially expressed genes in hip cartilage with femoral head necrosis, based on genome-wide expression profiles

WEN CHAO LI^{1*}, DE LEI BAI^{2*}, YANG XU^{3*}, RUI JIANG XU¹ and WEN BO HOU²

¹Department of Pediatric Surgery, Chinese People's Liberation Army General Hospital, Beijing 100853;

²Department of Orthopedics, Development Zones Center Hospital of Heze, Heze, Shandong 27400;

³Respiratory Department, Chinese People's Liberation Army General Hospital, Beijing 100853, P.R. China

Received July 15, 2018; Accepted January 7, 2019

DOI: 10.3892/mmr.2019.10458

Abstract. Necrosis of the femoral head (NFH), a severe orthopedic disease in adults, involves the collapse of the femoral head. The pathophysiological mechanisms underlying NFH are yet to be fully investigated. The aim of the present study was to identify potentially important genes and signaling pathways involved in NFH and investigate their molecular mechanisms. Gene expression profiles of patients with NFH and healthy controls were compared using the Gene Expression Omnibus (GEO) database repository of the National Center of Biotechnology Information. GSE74089 from the GEO database included 4 patients with NFH and 4 healthy individuals. A total of 1,191 differentially expressed genes (DEGs) were identified between the patients with NFH and controls, including 743 upregulated and 448 downregulated DEGs. Then, Gene Ontology and Kyoto Encyclopedia of Genes and Genomes pathway enrichment analysis revealed

that upregulated DEGs were mainly involved in the phosphoinositide 3-kinase/protein kinase B signaling pathway, focal adhesion and extracellular matrix-receptor interactions. Additionally, protein-protein interaction (PPI) analysis identified the most central DEGs as vascular endothelial growth factor A, Jun proto-oncogene, cyclin D1, fibroblast growth factor 2, HECT domain and ankyrin repeat-containing E3 ubiquitin protein ligase 1, protein kinase α , bone morphogenetic protein 2 and prostaglandin-endoperoxide synthase 2. PPI analysis also identified guanine nucleotide-binding protein, $\gamma 13$ as the most commonly downregulated gene based on different centrality. The results of the present study may provide novel insight into the genes and associated pathways involved in NFH, and aid the identification of novel therapeutic targets and biomarkers in the treatment of NFH.

Introduction

Necrosis of the femoral head (NFH) is a common disease of the hip, with a high incidence among elderly patients; the most common clinical symptom is severe pain (1). The pathological characteristics of NFH include reduced blood supply to the hip, collapse of the femoral head and microfracture accumulation without sustained remodeling (2,3). Early clinical symptoms may involve pain, ultimately leading to loss of movement in the hip (4). NFH is frequently treated by total hip arthroplasty in the end-stage of hip arthritis (5); however, the pathogenesis and molecular mechanisms underlying NFH remain unclear.

Numerous studies have focused on the etiology of NFH. Huang *et al* (6) reported that fibroblast growth factor 2 (FGF2) and family with sequence similarity 201 member A were associated with the development of NFH, and that insulin-like growth factor 1, SOX9 and collagen type II $\alpha 1$ may also affect the pathogenesis of NFH. The signal transducer and activator of transcription (STAT)1-caspase 3 pathway upregulated the expression of caspase 3, resulting in apoptosis in NFH (7). Tian *et al* (8) demonstrated that NFH was associated with the Toll-like receptor 4 signaling pathway, which may serve an important role in the pathogenesis of osteonecrosis. MicroRNAs (miRs) are also notable diagnostic markers and therapeutic targets of NFH. In a study by Li *et al* (9), has-miR-195-5p exhibited notable downregulation during the collapse of osteonecrotic femoral heads, suggesting that

Correspondence to: Professor Wen Chao Li, Department of Pediatric Surgery, Chinese People's Liberation Army General Hospital, 28 Fuxing Road, Haidian, Beijing 100853, P.R. China
E-mail: liwenchao301@163.com

*Contributed equally

Abbreviations: NFH, necrosis of the femoral head; NCBI, National Center of Biotechnology Information; GEO, gene expression omnibus; DEGs, differentially expressed genes; GO, Gene Ontology; STAT, signal transducer and activator of transcription; PPI, protein-protein interaction; DAVID, Database for Annotation, Visualization and Integrated Discovery; KEGG, Kyoto Encyclopedia of Genes and Genomes; BP, biological process; CC, cellular component; MF, molecular function; STRING, Search Tool for the Retrieval of Interacting Genes/Proteins; VEGFA, vascular endothelial growth factor A; GNG13, guanine nucleotide binding protein, $\gamma 13$; BMP, bone morphogenetic protein; AAV, adeno-associated virus; MAPK, mitogen-activated protein kinase; PAF, platelet activating factor; PAFR, platelet-activating factor receptor

Key words: differentially expressed gene, necrosis of femoral head, gene expression profiles, enrichment analysis, cartilage

the collapse may be associated with the downregulation of miR-195-5p. Wei *et al* (10) revealed that the long non-coding RNA Hox antisense intergenic RNA may inhibit miR-17-5p to regulate osteogenic differentiation and proliferation in the osteonecrosis of the femoral head. Ma *et al* (11) revealed that Runt-related transcription factor 2 and transcription factor Sp7 were downregulated in a rat model of NFH, whereas AJ18 was upregulated.

Microarray analysis using high-throughput platforms is a promising and efficient tool for the investigation of the molecular mechanisms of disease, and the identification of useful biomarkers for the diagnosis and prognosis of disease. Lin and Lin (12) reported 215 differentially expressed genes (DEGs) based on gene expression profiles generated from 3 steroid-induced samples from a rat model of NFH and 3 normal rat samples. Tong *et al* (13) revealed 190 DEGs in a rat model of NFH, 52 of which were upregulated and 138 downregulated. Biological functions identified from enrichment analysis of DEGs included signal transduction, apoptosis, extracellular matrix (ECM), angiogenesis and oxidative stress.

In the present study, DEGs were identified in patients with NFH, and associated pathways were analyzed to identify the underlying molecular mechanisms of this disease. Gene expression profiles in the cartilage of patients with NFH and healthy individuals were acquired from the National Center of Biotechnology Information (NCBI) Gene Expression Omnibus (GEO) database and compared. The GSE74089 microarray dataset was analyzed using R software, Bioconductor packages and the Database for Annotation, Visualization and Integrated Discovery (DAVID) 6.8 online resource. A protein-protein interaction (PPI) network of DEGs was then constructed in order to analyze the putative hub genes of NFH.

Materials and methods

Agilent microarray data processing and gene expression profile mining. The microarray data of GSE74089 (14) in NFH was obtained from the NCBI GEO database (15). GSE74089 contained data from cartilage samples from patients with NFH and healthy controls. The microarray data of GSE74089 were obtained using GPL13497 (Agilent-026652 Whole Human Genome Microarray 4x44K v2; Agilent Technologies, Inc., Santa Clara, CA, USA); the data were based on cartilage samples from 4 patients with NFH and 4 controls.

The pre-processing of gene expression profile data was performed using R software (version 3.4.0; <https://www.r-project.org>) and Bioconductor packages 3.8 (<https://www.bioconductor.org/>) for data analysis. Via the Agilent platform, R software was used to analyze the pre-processing and normalization of Series Matrix Files (.TXT files). The parameters used in the R software included robust multi-array average (for background correction), quantiles (for normalization), perfect match (PM)-only (PM correction) and median polish (as a summary measure).

Identification of DEGs. The Linear Models for Microarray Data 3.8 (LIMMA, <http://www.bioconductor.org/packages/release/bioc/html/limma.html>) package (16) in Bioconductor was employed to evaluate DEGs by comparing

the expression values in the cartilage of patients with NFH and controls. The corresponding P-value of gene symbols following a t-test was defined as the adjusted P-value; log₂ fold change >2 and P<0.01 were considered to be the cut-off criteria for DEGs.

Enrichment analysis of DEGs. DAVID 6.8 was employed for enrichment analysis, in order to investigate DEGs at the molecular and functional level (17,18). DAVID is a gene functional classification tool, which provides typical batch annotation and gene-Gene Ontology (GO) term enrichment analysis to highlight the most relevant GO terms associated with a specific gene list. DAVID was employed for GO function and Kyoto Encyclopedia of Genes and Genomes (KEGG) pathway enrichment analyses of DEGs in NFH (19-21). GO terms included 'cellular component (CC)', 'molecular function (MF)' and 'biological process (BP)'; P<0.05 was set as the cut-off for enrichment analysis.

Analysis of PPI networks. Search Tool for the Retrieval of Interacting Genes/Proteins (STRING; <http://string-db.org>) (22,23) is a database that predicts the PPIs of DEGs. According to the STRING database, PPIs of DEGs with a score (median confidence) of >0.4 were selected, and Cytoscape (Version 3.4.0, available online: <http://www.cytoscape.org/>) was used to analyze the PPI network (24). Hub-proteins are significant nodes of protein interaction within the PPI network (25). To characterize hubs in the PPI network of DEGs, betweenness centrality, degree centrality, Maximum Neighborhood Component (MNC) centrality and stress centrality were evaluated.

Results

Identification of DEGs in NFH. To identify DEGs in the cartilage of NFH and healthy patients, the transcription profile data of GSE74089 were obtained from the NCBI GEO database based on 4 patients with NFH and 4 healthy controls. According to the cut-off criteria, 1,191 DEGs were identified in the cartilage of patients with NFH compared with the controls, including 448 downregulated and 743 upregulated DEGs. DEGs in NFH samples were identified using hierarchical cluster analysis of the data (Fig. 1).

Enrichment analysis of DEGs. GO functional enrichment analysis revealed that the BPs of upregulated DEGs included 'ECM organization', '*in utero* embryonic development', 'collagen catabolic processes', 'collagen fibril organization' and 'angiogenesis' (Table I). CC analysis revealed that upregulated DEGs were primarily enriched in 'proteinaceous ECM', 'collagen trimer' and 'ECM'. The MFs of upregulated DEGs were demonstrated to include 'protein binding', 'platelet-derived growth factor binding', 'ubiquitin-protein transferase activity', 'ECM structural constituent' and 'oxidoreductase activity'. The BPs of downregulated DEGs included 'antigen processing and the presentation of peptide or polysaccharide antigen via major histocompatibility complex (MHC) class II', and 'immunoglobulin (Ig) production associated with Ig-mediated immune response', and 'antigen processing and presentation of exogenous peptide antigen via MHC class II'

Table I. Top 5 terms identified by GO enrichment analysis for the upregulated DEGs in necrosis of the femoral head samples.

Category	Term	Description	Count	P-value	Genes
BP	GO:0030574	Collagen catabolic process	14	2.87x10 ⁻⁷	COL18A1, COL13A1, COL3A1, COL15A1, COL2A1, MMP13, COL5A2, ...
	GO:0030198	Extracellular matrix organization	24	4.46x10 ⁻⁷	COL18A1, PXDN, COL13A1, LUM, COL3A1, CCDC80, DAG1, ...
	GO:0030199	Collagen fibril organization	11	6.94x10 ⁻⁷	LUM, TGFBR1, COL3A1, COL1A2, COL2A1, COL1A1, LOX, LOXL2, ...
	GO:0001701	In utero embryonic development	23	7.58x10 ⁻⁷	SRSF1, MAFF, CCM2, BMP2, ADAM10, TGFBR1, GJA1, UBR3, ...
	GO:0001525	Angiogenesis	23	1.38x10 ⁻⁵	PRKCA, SLC12A6, COL18A1, PTGS2, COL15A1, RORA, ECM1, THY1, ...
CC	GO:0031012	Extracellular matrix	37	3.37x10 ⁻¹¹	ASPN, PXDN, LTBP1, LUM, IGFBP7, COL3A1, POSTN, COL2A1, ...
	GO:0005578	Proteinaceous extracellular matrix	30	4.00x10 ⁻⁸	ASPN, CTHRC1, PXDN, LTBP1, AMTN, MAMDC2, LUM, POSTN, ...
	GO:0005581	Collagen trimer	17	7.43x10 ⁻⁸	COL18A1, CTHRC1, COL13A1, COL3A1, COL15A1, COL2A1, MMP13, ...
	GO:0070062	Extracellular exosome	141	1.05x10 ⁻⁶	S100A4, TSPO, RARRES1, FSTL1, AQP1, PNP, OGN, HMCN1, DYSF, ...
	GO:0005615	Extracellular space	80	1.20x10 ⁻⁶	S100A4, COPA, CTHRC1, PXDN, IGFBP7, FSTL1, POSTN, IL11, OGN, ...
MF	GO:0005515	Protein binding	361	2.83x10 ⁻⁷	S100A4, XRCC4, LTBP1, PTGS2, SNIP1, LEMD3, PTPN21, FSTL1, ...
	GO:0048407	Platelet-derived growth factor binding	6	1.80x10 ⁻⁵	COL3A1, COL1A2, COL6A1, COL2A1, COL1A1, COL5A1
	GO:0004842	Ubiquitin-protein transferase activity	28	2.64x10 ⁻⁵	KBTBD13, FEM1B, KLHL2, LNX1, ZYG11B, FBXW7, UBE2D2, KLHL24, ...
	GO:0005201	Extracellular matrix structural constituent	11	8.76x10 ⁻⁵	PXDN, LUM, COL3A1, COL1A2, COL15A1, COL2A1, VCAN, COL1A1, ...
	GO:0016641	Oxidoreductase activity	4	3.79x10 ⁻⁴	LOXL4, LOXL3, LOX, LOXL2

BP, biological process; CC, cellular compartment; DEG, differentially expressed genes; GO, Gene Ontology; MF, molecular function.

(Table II). Additionally, CC enrichment analysis revealed downregulated DEGs to be mainly associated with 'MHC class II protein complex', 'integral component of the luminal side of the endoplasmic reticulum membrane' and 'endocytic vesicle membrane'. The MFs of downregulated DEGs were

demonstrated to include 'MHC class II receptor activity', 'peptide antigen binding', 'MHC class II protein complex binding', 'monooxygenase activity' and 'N,N-dimethylaniline monooxygenase activity'. According to KEGG pathway enrichment analysis, the downregulated DEGs were mainly

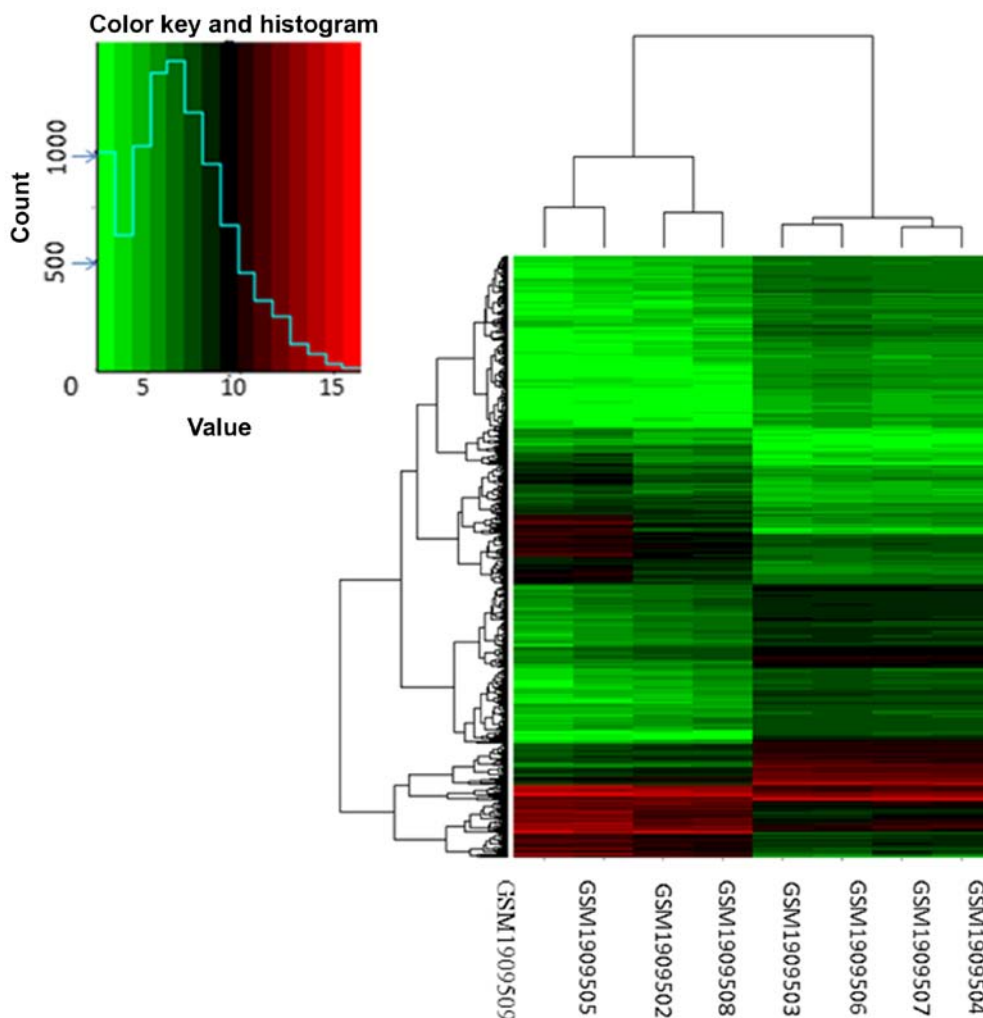


Figure 1. Heat map of DEGs in NFH. Tissue samples are presented as columns; individual genes are presented as rows. Green indicates upregulated genes and red indicates downregulated genes in patients with NFH. The patients in the right four columns (GSM1906503, 4, 6 and 7) were controls; the patients in the left four columns (GSM1909502, 3, 5 and 8) were patients with NFH. DEGs, differentially expressed genes; NFH, necrosis of the femoral head.

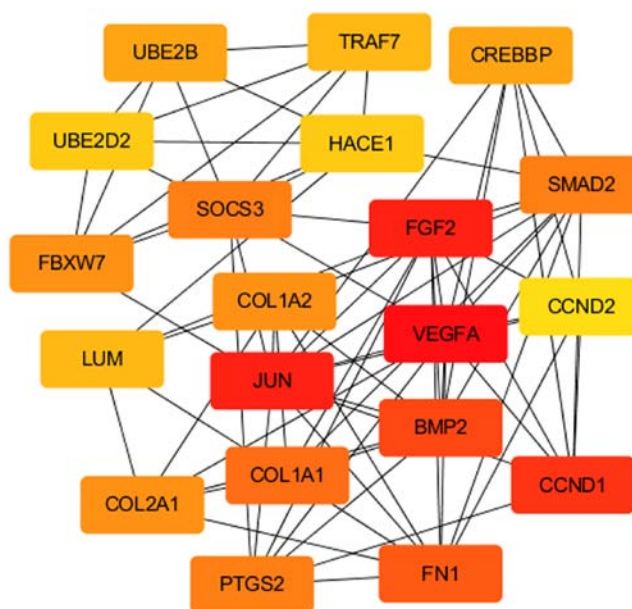


Figure 2. Module identified from the PPI network of the top 20 hub proteins of upregulated DEGs based on MNC centrality. The colors indicate the number of PPIs; red-labeled proteins exhibited an increased number of interactions compared with yellow-labeled proteins. DEGs, differentially expressed genes; MNC, Maximum Neighborhood Component; PPI, protein-protein interaction.

Table II. Top 5 terms identified by GO enrichment analysis for the downregulated DEGs in necrosis of the femoral head samples.

Category	Term	Description	Count	P-value	Genes
BP	GO:0002504	Antigen processing and presentation of peptide or polysaccharide antigen via MHC class II	9	8.90x10 ⁻¹¹	HLA-DQB1, HLA-DRB1, HLA-DRB3, HLA-DRB4, HLA-DRB5, ...
	GO:0002381	Immunoglobulin production involved in immunoglobulin mediated immune response	5	3.28x10 ⁻⁷	GAPT, HLA-DQB1, HLA-DRB1, HLA-DRB4, HLA-DRB5
	GO:0019882	Antigen processing and presentation	9	2.62x10 ⁻⁶	HLA-DQB1, HLA-DRB1, HLA-DRB3, HLA-DRB4, HLA-DRB5, ...
	GO:0019886	Antigen processing and presentation of exogenous peptide antigen via MHC class II	10	1.76x10 ⁻⁵	HLA-DQB1, HLA-DRB1, HLA-DRB3, SPTBN2, HLA-DRB4, ...
	GO:0060333	Interferon- γ -mediated signaling pathway	9	1.83x10 ⁻⁵	HLA-DQB1, HLA-DRB1, HLA-DRB3, HLA-DRB4, HLA-DRB5, ...
CC	GO:0042613	MHC class II protein complex	9	1.58x10 ⁻⁹	HLA-DQB1, HLA-DRB1, HLA-DRB3, HLA-DRB4, HLA-DRB5, ...
	GO:0071556	Integral component of luminal side of endoplasmic reticulum membrane	8	4.17x10 ⁻⁷	HLA-DQB1, HLA-DRB1, HLA-DRB3, HLA-DRB4, SPPL2B, ...
	GO:0030666	Endocytic vesicle membrane	9	1.49x10 ⁻⁵	HLA-DQB1, HLA-DRB1, HLA-DRB3, WNT3A, HLA-DRB4, ...
	GO:0012507	ER to Golgi transport vesicle membrane	8	2.56x10 ⁻⁵	HLA-DQB1, HLA-DRB1, FOLR1, HLA-DRB3, HLA-DRB4, ...
	GO:0030658	Transport vesicle membrane	7	3.89x10 ⁻⁵	HLA-DQB1, HLA-DRB1, HLA-DRB3, HLA-DRB4, HLA-DRB5, ...
MF	GO:0032395	MHC class II receptor activity	7	7.34x10 ⁻⁸	HLA-DQB1, HLA-DRB1, HLA-DRB3, HLA-DRB4, HLA-DOA, ...
	GO:0042605	Peptide antigen binding	7	4.63x10 ⁻⁶	HLA-DQB1, HLA-DRB1, HLA-DRB3, HLA-DRB4, HLA-DRB5, ...
	GO:0023026	MHC class II protein complex binding	4	0.001983	HLA-DRB1, HLA-DMB, HLA-DOA, HLA-DRA
	GO:0004497	Monoxygenase activity	6	0.00239	FMO1, FMO2, FMO6P, CYP4F22, CYP2E1, CYP4B1
	GO:0004499	N,N-dimethylaniline monoxygenase activity	3	0.003718	FMO1, FMO2, FMO6P

BP, biological process; CC, cellular compartment; DEG, differentially expressed genes; ER, endoplasmic reticulum; GO, Gene Ontology; MF, molecular function; MHC, major histocompatibility complex.

enriched in pathways involved in *staphylococcus aureus* infection, asthma and graft-versus-host disease. The upregulated DEGs were mainly enriched in pathways involved in focal adhesion, phosphoinositide 3-kinase (PI3K)/protein kinase B (Akt) signaling, pathways in cancer and ECM-receptor interactions (Table III).

PPI network analysis is important for understanding the biological responses of NFH. The STRING online database and Cytoscape software were employed to analyze the identified DEGs. The top 20 upregulated genes were evaluated for MNC centrality, betweenness centrality, stress centrality and degree centrality in the PPI network (Table IV). Based on various centrality, vascular endothelial growth factor A

(VEGFA) was the most notable gene in the PPI network. Jun proto-oncogene (JUN), cyclin D1 (CCND1), FGF2, HECT domain and ankyrin repeat-containing E3 ubiquitin protein ligase 1 (HACE1), protein kinase C α (PRKCA), bone morphogenetic protein (BMP) 2 and prostaglandin-endoperoxide synthase 2 (PTGS2) were within the top 5 genes of at least one of the centrality rankings. The significant network module generated based on MNC centrality is presented in Fig. 2. The top 15 downregulated DEGs were analyzed in the PPI network (Table V). Guanine nucleotide-binding protein, γ 13 (GNG13) was the most common gene based on various centrality. According to the MNC centrality, the significant network module is presented in Fig. 3.

Table III. Results of KEGG pathway enrichment analysis of differentially expressed genes.

Category	Term	Description	Count	P-value	Genes
Upregulated genes	hsa04510	Focal adhesion	28	1.44x10 ⁻⁸	COL3A1, COL2A1, ITGB8, SOS2, COL6A3, PPP1R12A, COL6A1, PDGFC, ...
	hsa04151	PI3K-Akt signaling pathway	33	2.29x10 ⁻⁶	PPP2R3A, STK11, COL3A1, COL2A1, GNG12, PKN3, ITGB8, SOS2, ...
	hsa04512	ECM-receptor interaction	14	2.24x10 ⁻⁵	COL3A1, DAG1, COL2A1, COL5A2, COL5A1, ITGB8, COL6A3, COL1A2, ...
	hsa04974	Protein digestion and absorption	14	2.54x10 ⁻⁵	COL18A1, COL13A1, SLC16A10, COL3A1, COL15A1, COL2A1, COL5A2, ...
	hsa05200	Pathways in cancer	31	1.96x10 ⁻⁴	GNAI3, ADCY7, PTGS2, EGLN3, BDKRB1, GNG12, GLI3, MMP1, GLI1, ...
Downregulated genes	hsa05150	Staphylococcus aureus infection	15	3.71x10 ⁻¹⁴	HLA-DQB1, C3AR1, HLA-DRB1, C4B, HLA-DRB3, HLA-DMB, ITGAM, ...
	hsa05310	Asthma	9	1.12x10 ⁻⁸	HLA-DQB1, HLA-DRB1, HLA-DRB3, HLA-DRB4, HLA-DRB5, HLA-DMB, ...
	hsa05332	Graft-versus-host disease	9	2.56x10 ⁻⁸	HLA-DQB1, HLA-DRB1, HLA-DRB3, HLA-DRB4, HLA-DRB5, HLA-DMB, ...
	hsa05330	Allograft rejection	9	6.76x10 ⁻⁸	HLA-DQB1, HLA-DRB1, HLA-DRB3, HLA-DRB4, HLA-DRB5, HLA-DMB, ...
	hsa04940	Type I diabetes mellitus	9	1.94x10 ⁻⁷	HLA-DQB1, HLA-DRB1, HLA-DRB3, HLA-DRB4, HLA-DRB5, HLA-DMB, ...

Akt, protein kinase B; ECM, extracellular matrix; KEGG, Kyoto Encyclopedia of Genes and Genomes; PI3K, phosphoinositide 3-kinase.

Discussion

NFH is a destructive bone disease, mainly induced by disruption of the blood supply and the dysfunction of the coagulation and fibrinolysis systems, which lead to the collapse of the femoral head (26,27). Various molecular and genetic studies have investigated the causes of the disease (28,29); however, the exact pathogenic mechanisms remain unclear. A genome-wide approach was employed to investigate differential gene expression in cartilage samples from patients with NFH and healthy controls. GSE74089 was analyzed to identify potentially important genes in NFH using bioinformatics analysis. The roles and interactions of the identified DEGs in NFH were also determined. A total of 1,191 DEGs were identified in cartilage samples from patients with NFH compared with the control, 448 of which were downregulated and 743 of which were upregulated. These DEGs may serve as important biomarkers with mechanistic relevance to the pathogenesis and progression of NFH.

The DEGs reported in the present study could aid the identification of novel molecules or pathways involved in NFH that may serve as targets in the diagnosis and treatment of the disease, and provide novel insight into its pathogenesis. Upregulated DEGs were involved in the organization of the ECM, collagen catabolism and fibril organization, *in utero* embryonic development and angiogenesis. The genes were mainly enriched in proteinaceous ECM, ECM and collagen trimers for CC enrichment. Liu *et al* (14), the study in which the GSE47089 microarray data were obtained, reported that DEGs in NFH were enriched in growth factors, cytokines, and proteins involved in cell cycle, platelet-derived growth factor binding, the ECM and apoptosis; these DEGs were enriched in collagen, the ECM and extracellular regions and platelet-derived growth factor binding. These findings were consistent with the results of the present study. Upregulated DEGs were mainly involved in PI3K-Akt signaling pathway, focal adhesion and ECM-receptor interactions. Downregulated DEGs were mainly enriched in pathways

Table IV. Evaluation of the top 20 upregulated DEGs of the protein-protein interaction network by MNC centrality, betweenness centrality, stress centrality and degree centrality.

Rank	MNC centrality	Betweenness centrality	Stress centrality	Degree centrality
1	VEGFA	VEGFA	VEGFA	VEGFA
2	JUN	CCND1	JUN	JUN
3	FGF2	JUN	CCND1	FGF2
4	CCND1	PRKCA	FGF2	CCND1
5	BMP2	PTGS2	HACE1	HACE1
6	FN1	FGF2	PTGS2	BMP2
7	COL1A1	HACE1	PRKCA	FN1
8	PTGS2	CREBBP	SMAD2	PTGS2
9	SMAD2	SMAD2	FN1	COL1A1
10	SOCS3	FN1	BMP2	SMAD2
11	COL2A1	BMP2	CREBBP	CREBBP
12	FBXW7	CD55	LUM	SOCS3
13	COL1A2	SOCS3	SOCS3	COL2A1
14	CREBBP	TJP1	JAK2	FBXW7
15	UBE2B	LUM	CDK9	PRKCA
16	LUM	JAK2	NT5E	UBE2B
17	TRAF7	NOTCH3	TGFBR1	LUM
18	HACE1	TGFBR1	NOTCH3	UBE2N
19	UBE2D2	NT5E	GNAI3	COL1A2
20	GNAI3	CDK9	CD55	GNAI3

DEG, differentially expressed genes; MNC, Maximum Neighborhood Component.

Table V. Evaluation of the top 15 downregulated DEGs of the protein-protein interaction network by MNC centrality, betweenness centrality, stress centrality and degree centrality.

Rank	MNC centrality	Betweenness centrality	Stress centrality	Degree centrality
1	GNG13	GNG13	PTAFR	GNG13
2	GNG8	PTAFR	GNG13	GNG8
3	SAA1	CTSH	CTSH	SAA1
4	CXCR1	SFTPBP	HLA-DRA	PTAFR
5	OPRL1	HLA-DRA	HLA-DRB5	HLA-DRA
6	C3AR1	HLA-DRB5	HLA-DRB1	HLA-DRB5
7	CORT	HLA-DRB1	SFTPBP	HLA-DRB1
8	PPYR1	TYROBP	GNG8	CXCR1
9	HTR1B	GNG8	SAA1	TYROBP
10	PTAFR	C1QB	SPTBN2	OPRL1
11	XCR1	SPTBN2	TYROBP	C3AR1
12	GHSR	SAA1	XCR1	CORT
13	LTB4R2	ITGAM	C1QB	PPYR1
14	HLA-DRA	XCR1	ITGAM	HTR1B
15	HLA-DRB5	CD163	CD163	XCR1

DEG, differentially expressed genes; MNC, Maximum Neighborhood Component.

involved in *staphylococcus aureus* infection, asthma and graft-versus-host disease. Focal adhesion kinase (FAK) is a non-receptor tyrosine kinase associated with a number of

different signaling proteins (30). Zhang *et al* (31) reported that CXC chemokine ligand 13 (CXCL13)/CXC chemokine receptor 5 (CXCR5)/FAK signaling is involved in the

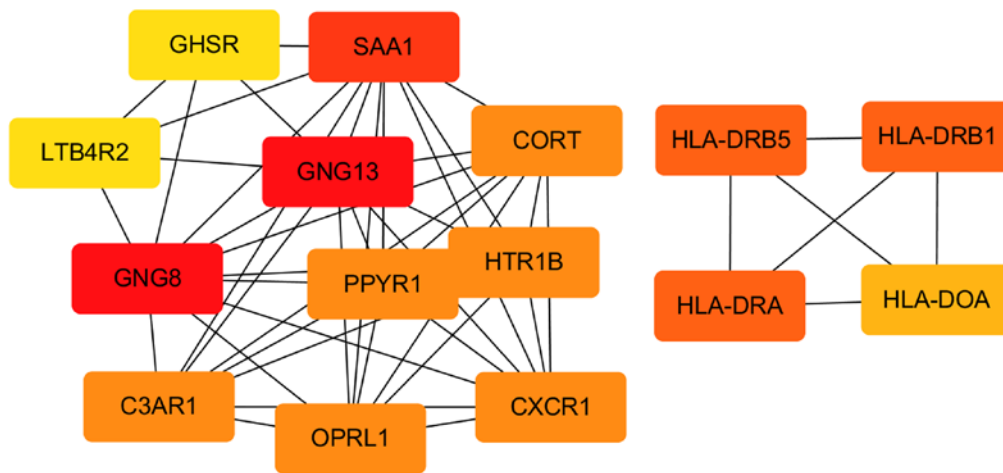


Figure 3. Module identified from the PPI network of the top 15 hub proteins of downregulated DEGs based on MNC centrality. The colors indicate the number of PPIs; red-labeled proteins exhibited an increased number of interactions compared with yellow-labeled proteins. DEGs, differentially expressed genes; MNC, Maximum Neighborhood Component; PPI, protein-protein interaction.

differentiation and trafficking of bone marrow stromal cells (BMSCs) in NFH; CXCL13/CXCR5 signaling was proposed to induce the phosphorylation of FAK via the mitogen-activated protein kinase (MAPK) pathway (32). The PI3K/Akt pathway is associated with various fundamental cellular processes, including survival, proliferation, growth and differentiation (33). Xue *et al.* (34) reported that Salidroside alleviated the dexamethasone-induced apoptosis of osteoblasts by downregulating caspase-3 and activating the PI3K/Akt signaling pathway in osteoblasts. In addition, the osteogenic differentiation-inducing and bone regenerative properties of graphene-incorporated poly(lactic-co-glycolic acid) were mediated via the activation of the PI3K/Akt/glycogen synthase kinase β / β -catenin signaling pathway (35).

PPI networks of DEGs were constructed using STRING and Cytoscape to investigate the associations between important proteins identified by GO enrichment and pathway analyses (36). The upregulated DEGs included VEGFA, JUN, CCND1, FGF2, HACE1, PRKCA, BMP2 and PTGS2. In the early stages of a rabbit model of NFH, BMP and VEGF were co-expressed using an adeno-associated virus (AAV) vector; the AAV-VEGF/BMP vector increased the bone repair capacity of the femoral head by inducing angiogenesis and improving bone quality (37). VEGF-expressing transgenic autologous BMSCs improved bone reconstruction and blood vessel regeneration in a canine model of NFH (38). Adenovirus-mediated expression of BMP2 and basic FGF in BMSCs in combination with a demineralized bone matrix improved bone formation in a dog model of NFH (39). CCND1 is an important regulatory factor of the cell cycle and is a frequently used biomarker for the diagnosis and prognosis of human primary tumors (40). Phosphorylated CCND1 is associated with the development of osteosarcoma, which may occur via MAPK-induced expression of CCND1, and the continuous proliferation of tumor cells (41).

Downregulated DEGs identified in the present study included GNG13, platelet-activating factor receptor (PAFR), GNG8, serum amyloid A1 and cathepsin H. PPI analysis identified GNG13 as a central downregulated DEG. GNG13 is a divergent member of the GNG subunit γ family and

contains a C-terminal NPW tripeptide (42). It is a component of the gustducin G-protein heterotrimer involved in bitter and sweet taste reception in taste bud cells (42). PAF is a potent phospholipid regulator of inflammation; PAFR is expressed on plasma and nuclear membranes in various cell types, and binds to PAF and oxidized phospholipids (43). Activation of PAFR in macrophages induces an anti-inflammatory phenotype (44). PAF activates PAFR, which may serve an important role in the malignant development of esophageal squamous cell carcinoma by stimulating PI3K/AKT activation, and promoting disease progression and metastasis via the initiation of a forward feedback loop between PAFR and STAT3 (45).

There were certain limitations to the present study. Gene expression data were obtained from only a single dataset containing 4 patients with NFH and 4 controls. The use of additional datasets with increased sample sizes in future studies would increase the accuracy and reliability of identified DEGs. Additionally, the potential role of DEGs and PPIs identified in the hip cartilage of patients with NFH require further investigation *in vivo* and *in vitro*; for example, the effects of silencing or upregulating DEGs in cellular or *in vivo* models could be determined. Furthermore, the altered expression of genes and proteins identified by microarray analysis should be investigated via reverse transcription-quantitative polymerase chain reaction and histological analyses of samples from patients with NFH. These experiments may validate the diagnostic and prognostic potential of identified DEGs for the disease.

In conclusion, following integrated bioinformatical analysis of the gene expression profiles of cartilage from patients with NFH and controls, 1,191 DEGs were identified in necrotic samples, 743 of which were upregulated and 448 were downregulated. DEG enrichment analysis identified molecules and pathways, which may provide novel insight into the pathogenesis of NFH. PPI network analysis identified VEGFA, JUN, CCND1, FGF2, HACE1, PRKCA, BMP2 and PTGS2, and GNG13 as central upregulated and downregulated DEGs, respectively. These DEGs and signaling pathways may serve as biomarkers and targets in the treatment of NFH; however, further investigation is required.

Acknowledgements

Not applicable.

Funding

This study was supported by Clinical Support Foundation of Chinese PLA General Hospital (grant nos. 2017FC-TSYS-3015 and 2017FC-TSYS-2043), Nursery Foundation of Chinese PLA General Hospital (grant no. 17KMM12), Beijing Natural Science Foundation (grant no. 7192196) and National Natural Science Foundation of China (grant no. 81702169).

Availability of data and materials

The datasets used and/or analyzed during the present study are available from the corresponding author on reasonable request.

Authors' contributions

WCL made substantial contributions towards the conception and design of the study, and experiments. DLB and YX performed the major bioinformatics analysis of the gene database. RJX and WBH performed the analysis of DEGs. WCL drafted the manuscript, aggregated the figures and discussed the results. RJX contributed to the revision of the manuscript.

Ethics approval and consent to participate

Not applicable.

Patient consent for publication

Not applicable.

Competing interests

The authors declare that they have no competing interests.

References

- Zhang QY, Li ZR, Gao FQ and Sun W: Pericollaps stage of osteonecrosis of the femoral Head: A last chance for joint preservation. *Chin Med J (Engl)* 131: 2589-2598, 2018.
- Hauzeur JP, Malaise M and de Maertelaer V: A prospective cohort study of the clinical presentation of non-traumatic osteonecrosis of the femoral head: Spine and knee symptoms as clinical presentation of hip osteonecrosis. *Int Orthop* 40: 1347-1351, 2016.
- Moya-Angeler J, Gianakos AL, Villa JC, Ni A and Lane JM: Current concepts on osteonecrosis of the femoral head. *World J Orthop* 6: 590-601, 2015.
- Shah KN, Racine J, Jones LC and Aaron RK: Pathophysiology and risk factors for osteonecrosis. *Curr Rev Musculoskelet Med* 8: 201-209, 2015.
- Al-Khateeb H, Kwok IH, Hanna SA, Sewell MD and Hashemi-Nejad A: Custom cementless THA in patients with legg-calve-perthes disease. *J Arthroplasty* 29: 792-796, 2014.
- Huang G, Zhao G, Xia J, Wei Y, Chen F, Chen J and Shi J: FGF2 and FAM201A affect the development of osteonecrosis of the femoral head after femoral neck fracture. *Gene* 652: 39-47, 2018.
- Xu X, Wen H, Hu Y, Yu H, Zhang Y, Chen C and Pan X: STAT1-caspase 3 pathway in the apoptotic process associated with steroid-induced necrosis of the femoral head. *J Mol Histol* 45: 473-485, 2014.
- Tian L, Wen Q, Dang X, You W, Fan L and Wang K: Immune response associated with Toll-like receptor 4 signaling pathway leads to steroid-induced femoral head osteonecrosis. *BMC Musculoskelet Disord* 15: 18, 2014.
- Li P, Zhai P, Ye Z, Deng P, Fan Y, Zeng Y, Pang Z, Zeng J, Li J and Feng W: Differential expression of miR-195-5p in collapse of steroid-induced osteonecrosis of the femoral head. *Oncotarget* 8: 42638-42647, 2017.
- Wei B, Wei W, Zhao B, Guo X and Liu S: Long non-coding RNA HOTAIR inhibits miR-17-5p to regulate osteogenic differentiation and proliferation in non-traumatic osteonecrosis of femoral head. *PLoS One* 12: e0169097, 2017.
- Ma XL, Liu ZP, Ma JX, Han C and Zang JC: Dynamic expression of Runx2, Osterix and AJ18 in the femoral head of steroid-induced osteonecrosis in rats. *Orthop Surg* 2: 278-284, 2010.
- Lin Z and Lin Y: Identification of potential crucial genes associated with steroid-induced necrosis of femoral head based on gene expression profile. *Gene* 627: 322-326, 2017.
- Tong P, Wu C, Jin H, Mao Q, Yu N, Holz JD, Shan L, Liu H and Xiao L: Gene expression profile of steroid-induced necrosis of femoral head of rats. *Calcif Tissue Int* 89: 271-284, 2011.
- Liu R, Liu Q, Wang K, Dang X and Zhang F: Comparative analysis of gene expression profiles in normal hip human cartilage and cartilage from patients with necrosis of the femoral head. *Arthritis Res Ther* 18: 98, 2016.
- Barrett T, Wilhite SE, Ledoux P, Evangelista C, Kim IF, Tomashevsky M, Marshall KA, Phillippy KH, Sherman PM, Holko M, *et al*: NCBI GEO: archive for functional genomics data sets-update. *Nucleic Acids Res* 41: D991-D995, 2013.
- Ritchie ME, Phipson B, Wu D, Hu Y, Law CW, Shi W and Smyth GK: limma powers differential expression analyses for RNA-sequencing and microarray studies. *Nucleic Acids Res* 43: e47, 2015.
- Huang da W, Sherman BT and Lempicki RA: Systematic and integrative analysis of large gene lists using DAVID bioinformatics resources. *Nat Protoc* 4: 44-57, 2009.
- Huang da W, Sherman BT and Lempicki RA: Bioinformatics enrichment tools: Paths toward the comprehensive functional analysis of large gene lists. *Nucleic Acids Res* 37: 1-13, 2009.
- Kanehisa M, Sato Y, Furumichi M, Morishima K and Tanabe M: New approach for understanding genome variations in KEGG. *Nucleic Acids Res* 47: D590-D595, 2019.
- Kanehisa M, Furumichi M, Tanabe M, Sato Y and Morishima K: KEGG: New perspectives on genomes, pathways, diseases and drugs. *Nucleic Acids Res* 45: D353-D361, 2017.
- Kanehisa M and Goto S: KEGG: Kyoto encyclopedia of genes and genomes. *Nucleic Acids Res* 28: 27-30, 2000.
- Szklarczyk D, Franceschini A, Wyder S, Forslund K, Heller D, Huerta-Cepas J, Simonovic M, Roth A, Santos A, Tsafou KP, *et al*: STRING v10: Protein-protein interaction networks, integrated over the tree of life. *Nucleic Acids Res* 43: D447-D452, 2015.
- Jensen LJ, Kuhn M, Stark M, Chaffron S, Creevey C, Muller J, Doerks T, Julien P, Roth A, Simonovic M, *et al*: STRING 8-a global view on proteins and their functional interactions in 630 organisms. *Nucleic Acids Res* 37: D412-D416, 2009.
- Shannon P, Markiel A, Ozier O, Baliga NS, Wang JT, Ramage D, Amin N, Schwikowski B and Ideker T: Cytoscape: A software environment for integrated models of biomolecular interaction networks. *Genome Res* 13: 2498-2504, 2003.
- Bertolazzi P, Bock ME and Guerra C: On the functional and structural characterization of hubs in protein-protein interaction networks. *Biotechnol Adv* 31: 274-286, 2013.
- Li Z, Yang B, Weng X, Tse G, Chan MTV and Wu WKK: Emerging roles of MicroRNAs in osteonecrosis of the femoral head. *Cell Prolif* 51, 2018.
- Cohen-Rosenblum A and Cui Q: Osteonecrosis of the femoral Head. *Orthop Clin North Am* 50: 139-149, 2019.
- Wei B and Wei W: Identification of aberrantly expressed of serum microRNAs in patients with hormone-induced non-traumatic osteonecrosis of the femoral head. *Biomed Pharmacother* 75: 191-195, 2015.
- Song Y, Du ZW, Yang QW, Ren M, Wang QY, Wang A, Chen GY, Zhao HY, Yu T and Zhang GZ: Association of genes variants in RANKL/RANK/OPG signaling pathway with the development of osteonecrosis of the femoral head in Chinese population. *Int J Med Sci* 14: 690-697, 2017.
- Peng X and Guan JL: Focal adhesion kinase: From in vitro studies to functional analyses in vivo. *Curr Protein Pept Sci* 12: 52-67, 2011.
- Zhang Y, Ma C, Yu Y, Liu M and Yi C: Are CXCL13/CXCR5/FAK critical regulators of MSCs migration and differentiation? *Med Hypotheses* 84: 213-215, 2015.

32. MacDonald RJ and Yen A: CXCR5 overexpression in HL-60 cells enhances chemotaxis toward CXCL13 without anticipated interaction partners or enhanced MAPK signaling. *In Vitro Cell Dev Biol Anim* 54: 725-735, 2018.
33. Gu YX, Du J, Si MS, Mo JJ, Qiao SC and Lai HC: The roles of PI3K/Akt signaling pathway in regulating MC3T3-E1 preosteoblast proliferation and differentiation on SLA and SLActive titanium surfaces. *J Biomed Mater Res A* 101: 748-754, 2013.
34. Xue XH, Feng ZH, Li ZX and Pan XY: Salidroside inhibits steroid-induced avascular necrosis of the femoral head via the PI3K/Akt signaling pathway: *In vitro* and *in vivo* studies. *Mol Med Rep* 17: 3751-3757, 2018.
35. Wu X, Zheng S, Ye Y, Wu Y, Lin K and Su J: Enhanced osteogenic differentiation and bone regeneration of poly(lactic-co-glycolic acid) by graphene via activation of PI3K/Akt/GSK-3 β / β -catenin signal circuit. *Biomater Sci* 6: 1147-1158, 2018.
36. Aki T, Hashimoto K, Ogasawara M and Itoi E: A whole-genome transcriptome analysis of articular chondrocytes in secondary osteoarthritis of the hip. *PLoS One* 13: e0199734, 2018.
37. Zhang C, Ma J, Li M, Li XH, Dang XQ and Wang KZ: Repair effect of coexpression of the hVEGF and hBMP genes via an adeno-associated virus vector in a rabbit model of early steroid-induced avascular necrosis of the femoral head. *Transl Res* 166: 269-280, 2015.
38. Hang D, Wang Q, Guo C, Chen Z and Yan Z: Treatment of osteonecrosis of the femoral head with VEGF165 transgenic bone marrow mesenchymal stem cells in mongrel dogs. *Cells Tissues Organs* 195: 495-506, 2012.
39. Peng WX and Wang L: Adenovirus-mediated expression of BMP-2 and BFGF in bone marrow mesenchymal stem cells combined with demineralized bone matrix for repair of femoral head osteonecrosis in beagle dogs. *Cell Physiol Biochem* 43: 1648-1662, 2017.
40. Xu J and Lin DI: Oncogenic c-terminal cyclin D1 (CCND1) mutations are enriched in endometrioid endometrial adenocarcinomas. *PLoS One* 13: e0199688, 2018.
41. Wu J, Cui LL, Yuan J, Wang Y and Song S: Clinical significance of the phosphorylation of MAPK and protein expression of cyclin D1 in human osteosarcoma tissues. *Mol Med Rep* 15: 2303-2307, 2017.
42. Blake BL, Wing MR, Zhou JY, Lei Q, Hillmann JR, Behe CI, Morris RA, Harden TK, Bayliss DA, Miller RJ and Siderovski DP: G beta association and effector interaction selectivities of the divergent G gamma subunit G gamma(13). *J Biol Chem* 276: 49267-49274, 2001.
43. da Silva Junior IA, de Sousa Andrade LN, Jancar S and Chammas R: Platelet activating factor receptor antagonists improve the efficacy of experimental chemo- and radiotherapy. *Clinics (Sao Paulo)* 73 (Suppl 1): e792s, 2018.
44. Filgueiras LR, Koga MM, Quaresma PG, Ishizuka EK, Montes MB, Prada PO, Saad MJ, Jancar S and Rios FJ: PAFR in adipose tissue macrophages is associated with anti-inflammatory phenotype and metabolic homeostasis. *Clin Sci (Lond)* 130: 601-612, 2016.
45. Chen J, Lan T, Zhang W, Dong L, Kang N, Zhang S, Fu M, Liu B, Liu K, Zhang C, *et al*: Platelet-activating factor receptor-mediated PI3K/AKT activation contributes to the malignant development of esophageal squamous cell carcinoma. *Oncogene* 34: 5114-5127, 2015.



This work is licensed under a Creative Commons Attribution-NonCommercial-NoDerivatives 4.0 International (CC BY-NC-ND 4.0) License.